Type I Interferon Signaling Is Critical During the Innate Immune Response to HSV-1 Retinal Infection

Shan Fan,[1] Jae Hyuk Yoo,[1,2] Garam Park,[1,2] Steven Yeh,[1] and Christopher D. Conrady[1,3]

[1]Department of Ophthalmology and Visual Sciences, Truhlsen Eye Center, University of Nebraska Medical Center, Omaha, Nebraska, United States
[2]Fred and Pamela Buffett Cancer Center, University of Nebraska Medical Center, Omaha, Nebraska, United States
[3]Department of Pathology and Microbiology, University of Nebraska Medical Center, Omaha, Nebraska, United States

Correspondence: Christopher D. Conrady, Assistant Professor of Ophthalmology and Pathology and Microbiology, Truhlsen Eye Institute, University of Nebraska Medical Center, 3902 Leavenworth St., Omaha, NE 68105, USA; cconrady@unmc.edu.

Received: September 22, 2022
Accepted: December 10, 2022
Published: December 30, 2022

Citation: Fan S, Yoo JH, Park G, Yeh S, Conrady CD. Type I interferon signaling is critical during the innate immune response to HSV-1 retinal infection. *Invest Ophthalmol Vis Sci.* 2022;63(13):28. https://doi.org/10.1167/iovs.63.13.28

Purpose. Acute retinal necrosis (ARN) is a herpesvirus infection of the retina with blinding complications. In this study, we sought to create a reproducible mouse model of ARN that mimics human disease to better understand innate immunity within the retina during virus infection.

Methods. C57Bl/6J wild type (WT) and type I interferon receptor–deficient ($IFNAR^{-/-}$) mice were infected with varying amounts of herpes simplex virus type 1 (HSV-1) via subretinal injection. Viral titers, optical coherence tomography (OCT) and fundus photography, the development of encephalitis, and ocular histopathology were scored and compared between groups of WT and $IFNAR^{-/-}$ mice.

Results. The retina of WT mice could be readily infected with HSV-1 via subretinal injection resulting in retinal whitening and full-thickness necrosis as determined by in vivo imaging and histopathology. In $IFNAR^{-/-}$ mice, HSV-1-induced retinal pathology was significantly worse when compared with WT mice, and viral titers were significantly elevated within two days after infection and persisted to day 5 after infection within the retina. These results were also observed in the brain where there were significantly higher viral titers and frequency of encephalitis in $IFNAR^{-/-}$ when compared to WT mice.

Conclusions. Collectively, these findings show that our new mouse model of ARN mimics human disease and can be used to study innate immunity within the retina. We conclude that type I interferons are critical in containing HSV-1 locally within retinal tissues and prohibiting spread into the brain.

Keywords: acute retinal necrosis, innate immunity, eye, infection, type I interferons

Herpesviruses cause a spectrum of disease in humans ranging from recurrent cold sores to death from encephalitis.[1] Acute retinal necrosis (ARN) is a herpes virus infection of the retina that causes irreversible tissue destruction and occlusive vasculitis resulting in permanent vision loss and high rates of recurring retinal detachments in children and adults.[2] Long-term visual outcomes are poor, with a mean visual acuity of 20/400 in children despite aggressive treatment.[3] Herpes simplex virus (HSV) type 1, HSV-2, or varicella zoster virus are the most common causes of ARN.[4] The disease is typically unilateral; however, bilateral cases are not uncommon with associated clinical or subclinical encephalitis.[5] Samples from patients with ARN have shown a broad upregulation of cytokines and chemokines within the aqueous and vitreous fluid of the eye and blood.[6,7] This upregulation of systemic inflammatory markers and association with encephalitis suggest a broader host-pathogen interaction than simply within the eye. Consequently, a better understanding of ARN pathogenesis may improve both visual and cognitive outcomes.

Our current understanding of ARN is derived from vitreous samples and mouse models of disease. Previously, mouse models of ARN have used intracameral injections of Kendall O. Smith (KOS) strain HSV-1 into the anterior chamber of BALB/c mice with the virus subsequently spreading through synaptically-connected neurons to the contralateral optic nerve and retina resulting in a necrotizing retinitis reminiscent of human disease (von Szily model).[8,9] The innate immune response that drives the production of inflammatory chemokines and cytokines and antiviral compounds such as type I interferons (IFN) within the retina is currently unknown in both mice and humans; however, we do know that type I and II interferons are rapidly produced after HSV infection within the eye.[10] Unfortunately, the use of the von Szily model is limited by the background of mice (BALB/c mice with few available innate knockout strains) and precise timing of retinal infection making the study of the innate immune response within the retina difficult. Furthermore, the clinical presentation varies from that typically seen in humans in which only one eye is typically affected, and preceding inflammation in the fellow eye is uncommon.[11,12] As such, we adapted an ARN model from rabbits and retinal detachment model in mice in which HSV-1 is injected directly into the subretinal space to more closely resemble human disease, provide a better, more controlled model, and limit inflammation to bystander tissues to under-

Copyright 2022 The Authors

This work is licensed under a Creative Commons Attribution-NonCommercial-NoDerivatives 4.0 International License.

stand the earliest immune response to the virus specifically within the retina.[13,14]

Based off of our current understanding of the importance of type I IFN in other tissues,[15–18] we hypothesized that the loss of type I IFN signaling would result in rapid viral spread into the central nervous system and worse destruction of host retinal tissue using our mouse model of acute retinal necrosis. In the following study, we found that the loss of type I IFN signaling resulted in loss of local viral containment and destruction of host tissue.

Methods

Mice and Virus

C57BL/6J wild type (WT) and IFNAR$^{-/-}$ mice were purchased from Jackson Laboratory and housed in UNMC's animal facility. All mice were age- and sex-matched and were between six and eight weeks old at the time of the experiment. Animal treatment was consistent with the National Institutes of Health Guidelines on the Care and Use of Laboratory Animals and adhered to the Association for Research in Vision and Ophthalmology conduct for use of animal models. All experimental procedures were approved by the University of Nebraska Medical Center's Institutional Animal and Care Use Committee. Institutional review board approval was not needed for a single, deidentified image. HSV-1 McKrae was propagated in Vero cells and maintained at a stock concentration of 10^8 plaque forming units (PFU)/mL. Mouse pupils were then dilated with topical tropicamide and phenylephrine. A sclerotomy using a 27-gauge needle was made in anesthetized mice as previously described. Using an ophthalmic surgical microscope and cornea contact lens, mice were infected with 100 to 10,000 PFU of HSV-1 diluted in sterile PBS by injection into the subretinal space of mice through a 36-gauge beveled needle. Subretinal injection of PBS was considered a negative control. Retinal tissue and the cerebrum were then isolated at the indicated time. For plaque assays, at the indicated time post-infection (pi), tissue and cells were isolated, suspended in 500 µL of RPMI media, and homogenized with a tissue homogenizer for approximately 10 to 15 seconds. Media was clarified of cellular debris by centrifugation for two minutes at 10,000*g*. Infectious content within the clarified supernatant was then evaluated as previously described on Vero cells.[15]

In Vivo Imaging

Mice were anesthetized, the pupils were dilated with tropicamide and phenylephrine, and then fundus photography or OCT imaging was performed using a Heidelberg Spectralis and contact lens.

Immunohistochemical Staining and Confocal Imaging

Mice were euthanized, and eyes removed and fixed in 4% paraformaldehyde. Samples were then embedded in paraffin blocks, and 10 µm sections were cut and mounted on slides. Sections were then subjected to de-paraffinization and either H&E staining or blocked overnight at 4°C with blocking buffer (Thermo Fisher Scientific, Waltham, MA, USA). Samples to be evaluated by confocal microscopy were then subjected to an overnight incubation at 4°C with Iba-1 (Abcam, Cambridge, MA, USA) and anti-HSV-1 (Invitrogen, Carlsbad, CA, USA). The tissue was then washed three times and subjected to fluorescently-labeled secondary antibodies (Abcam) overnight at 4°C. Slides were then washed three more times, DAPI was applied, and imaged with a Zeiss 700 confocal microscope (Zeiss, Oberkochen, Germany). Pathological scoring was performed with a masked examiner adapting a previously validated grading system for mouse cytomegalovirus retinitis as detailed in the Table on H&E samples.[19]

Chemokine Analysis

Retinas were isolated from infected and uninfected mice as described above at the indicated time point after the procedure. Tissue was resuspended in RPMI and then homoge-

Table. Adapted ARN Histopathological Scoring System

Anterior Segment		
0	Normal	
1	Mild	Inflammatory cells but minimal HSV inclusions of iris and CB
2	Moderate	Inflammation and few HSV inclusions of iris and CB, minimal necrosis
3	Severe	Significant HSV inclusions cysts and/or necrosis of <1/2 of iris or CB
4	Extreme	Profound HSV inclusions cysts and/or necrosis of >1/2 of the iris or CB
Posterior Segment (Retinopathy)		
0	Normal	Normal or injection artifact
1/2	Mild retinopathy	No HSV inclusions + retinal folds and/or vascular cuffing involving <3/4 of section
1	Moderate retinopathy	Mild atypical retinopathy involving >3/4 of section; *or* photoreceptor degeneration and mild retinal infiltration involving <1/4 of section without necrosis or inclusions
2	Mild necrotizing retinitis	Focal HSV inclusions + partial-thickness necrosis involving <1/4 of section
3	Moderate necrotizing retinitis	HSV Inclusions + full-thickness retinal necrosis involving 1/4 to 3/4 of the section
4	Severe necrotizing retinitis	HSV Inclusions + full-thickness necrosis involving the entire retina in the section

CB, ciliary body
Adapted from Dix et al.[19]

Investigative Ophthalmology & Visual Science

nized for 12 to 15 seconds. Samples were then evaluated by magnetic bead array (Millipore, Burlington, MA, USA) per manufacturer's protocol for CXCL1, CCL2, CXCL10, IL-6, IL-10, IL-12p70, MIP-1α, MIP-1β, IFN-γ, and TNF-α.

Western Blot

Tissues were lysed in ice-cold Pierce IP lysis buffer (Thermo Fisher Scientific; 25 mM HEPES, pH 7.4; 150 mM NaCl; 1% NP-40; 1 mM EDTA; 5% glycerol) with protease and phosphatase inhibitors (Halt cocktail; Thermo Fisher Scientific) and spun in a centrifuge for 10 minutes at 14,000 rpm, and the supernatants were used to determine protein concentrations by BCA assays (Thermo Fisher Scientific). Each well of an SDS polyacrylamide gel was loaded with an equal amount of protein, and electrophoresis was conducted using Mini-PROTEAN Tetra cells (Bio-Rad Life Science, Hercules, CA, USA). Bands were transferred to polyvinylidene difluoride (PVDF) membranes (Bio-Rad Life Science) using the Trans-Blot Turbo system (Bio-Rad Life Science). Blocking buffer was 5% non-fat dry milk in PBS with 0.1% Tween 20. Primary antibodies were diluted in blocking buffer, and membranes were incubated on a shaker overnight at 4°C. After washing, secondary antibodies were applied at room temperature for one hour. After washing, a chemiluminescent HRP substrate (Thermo Fisher Scientific) was applied, and images were developed on ChemiDoc imaging system (Bio-Rad Life Science).

Statistical Analysis

Statistical analysis was performed using Prism's one-way analysis of variance followed by an ad hoc Tukey's *t* test in experiments comparing more than two groups, whereas a Student *t* test was used to compare two variables. Significance was defined as a P value < 0.05 throughout.

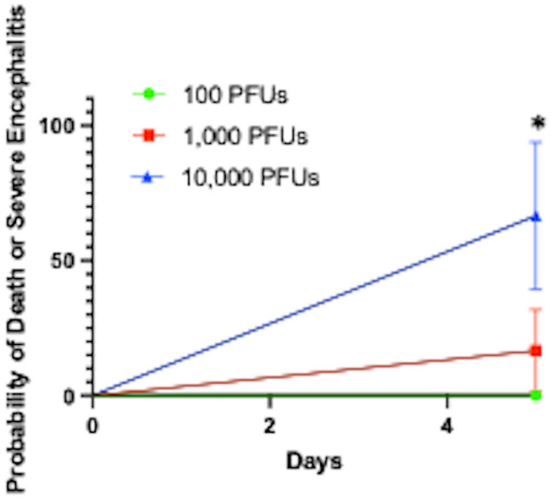

Figure 1. HSV-1 dose curve in WT mice. WT mice were infected with increasing concentrations of HSV-1 [100PFUs (*green line*), 1000 PFUs (*red line*), or 10,000 PFUs (*blue line*)] and probability of death or developing severe encephalitis recorded five days pi. Graph represents two independent experiments for a total of three to six mice per group (n = 3–6/group). $^{**}P < 0.05$.

Results

WT Mice Infected With Subretinal HSV-1 Develop Retinal Necrosis Reminiscent of Human Disease

To first assess whether the retina was permissive to direct infection with HSV-1, WT mice were injected with either a subretinal inoculum of PBS or increasing tenfold amounts of HSV-1 ranging from 10^2 to 10^4 infectious virus or input PFUs. The development of encephalitis as defined by previous grading criteria and mouse survival was then assessed

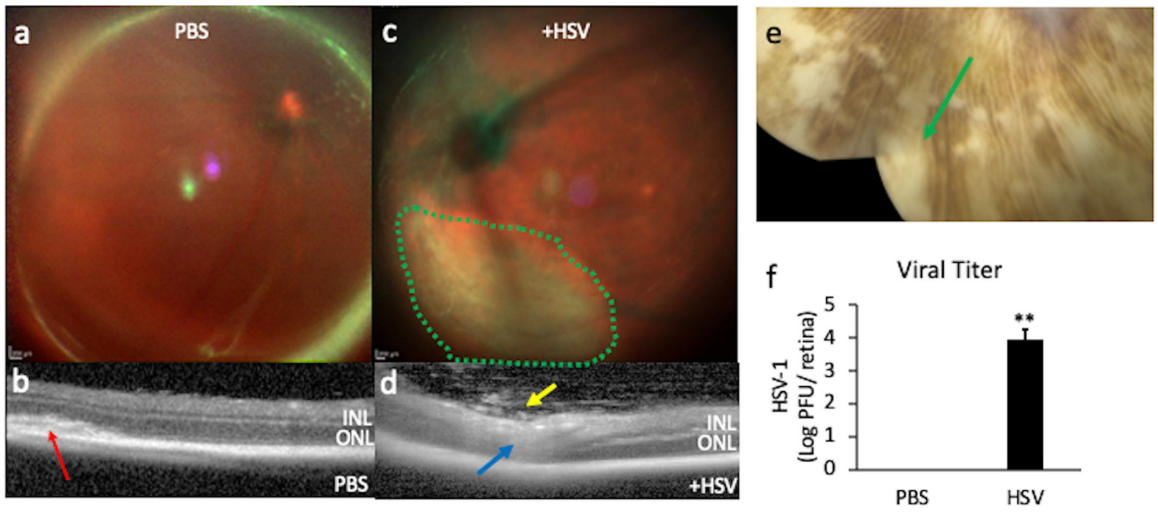

Figure 2. Retinal whitening, full-thickness necrosis, and replicating virus within WT mice five days pi. WT mice were subretinally injected with PBS or 1000 PFUs of HSV-1. At five days pi, fundus photography (**a, c**) and OCT imaging (**b, d**) were performed. HSV-1-infected mice showed retinal whitening (**c**, *green dotted line*), full-thickness necrosis (*blue arrow*) with overlying vitritis (*yellow arrow*) not seen in PBS controls. A small, residual subretinal bleb was occasionally seen five days after injection (*red arrow*). Retinal whitening appeared similar to that of the peripheral retina of a patient with HSV-1 PCR-proven ARN (*green arrow*, **e**). Five days pi, retinal tissue was evaluated for HSV-1 by plaque assay (**f**). Graph represents $\log_{10}$ PFUs/retina ± SEM of three independent experiments, n = 4-5/group. $^{**}P < 0.01$. INL, inner nuclear layer; ONL, outer nuclear layer.

Investigative Ophthalmology & Visual Science

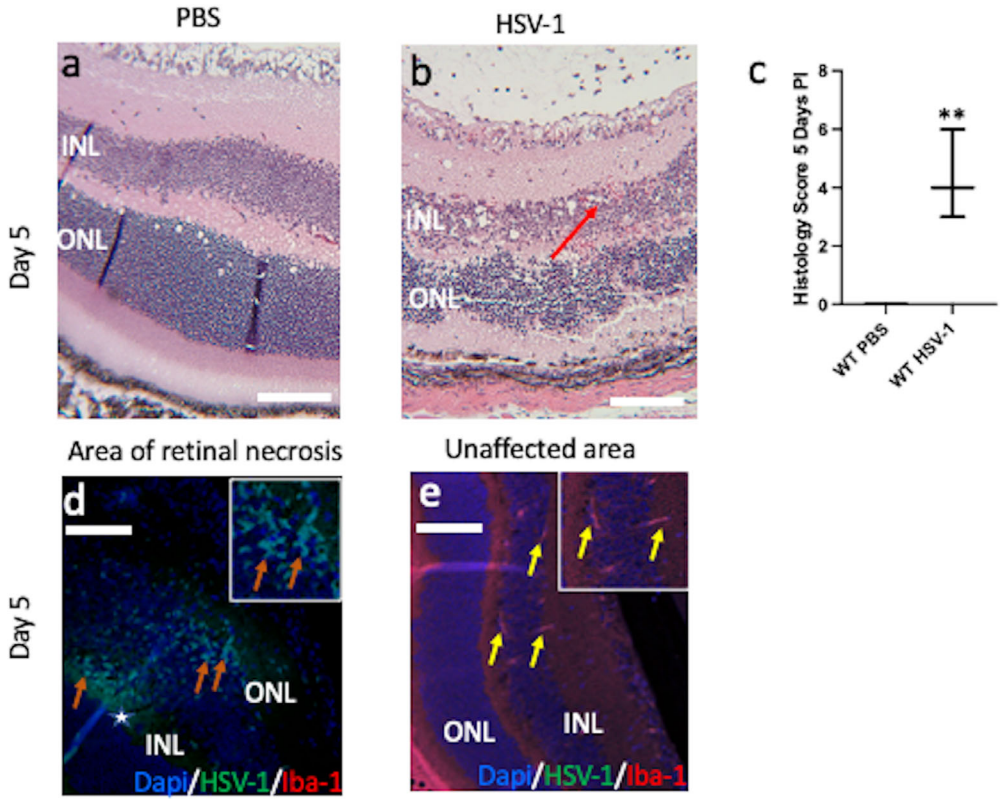

Figure 3. HSV-1 infection of the retina results in local tissue destruction. WT mice were subretinally injected with PBS or 1,000 PFUs of HSV-1. At five days pi, tissue was isolated, fixed, sectioned, and H&E stained. WT PBS controls retained good retinal architecture (**a**). Retinas from WT mice infected with HSV-1 showed intraretinal hemorrhages (*red arrow*), thinning of the inner and outer nuclear layers, overlying vitreous lymphocytes, and microglia within areas of tissue necrosis (**b**). Ocular pathology was then compared using a previously validated histology scoring system for retinitis (**c**). (**d, e**) Fluorescent imaging was then performed five days pi in WT mice. Images represent two independent experiments of two to four eyes/group. $^{**}P < 0.01$. INL, inner nuclear layer; ONL, outer nuclear layer; *White star*, area of HSV-1 antigen expression without colocalization; *orange arrows*, HSV-1 and Iba-1 colocalization; *yellow arrows*, Iba-1 positivity without HSV-1 expression; *white inset*, digital magnification of affected area. *White scale bars* are equal to 75 µm.

up to five days post infection (pi) (Fig. 1).[16] At day 5 pi, there was no mortality within WT mice and only one mouse developed any signs of encephalitis (Fig. 1). Because of significantly higher rates of severe morbidity at an infectious dose of 10^4 PFUs (two of three WT mice), we elected to use the highest dose of virus (10^3 PFU) that did not lead to mouse's demise at day 5 pi. WT mice injected with HSV-1 or sterile PBS were then serially imaged to affirm resolution of the subretinal inoculum and the development of retinal necrosis (Figs. 2a–d). Similar to that of human disease (Fig. 2e), WT mice infected with HSV-1 developed retinal whitening on fundus photography (green dotted line) and full-thickness retinal necrosis on in vivo OCT imaging (blue arrow) with overlying vitreous inflammation (yellow arrow) not seen in PBS controls (Figs. 2a–d). Mouse retinal tissue was permissive to HSV-1 infection because viable virus could be isolated from the tissue five days pi (Fig. 2f).

HSV-1 Infection of the Retina Results in Substantial Host Tissue Changes

To evaluate histopathological changes of the mouse retina, H&E staining was performed to affirm the in vivo findings with full-thickness necrosis, the development of Cowdry bodies (HSV-associated inclusion bodies) and intraretinal hemorrhages (red arrow), and substantial retinal architecture changes compared to PBS controls (Figs. 3a, 3b).

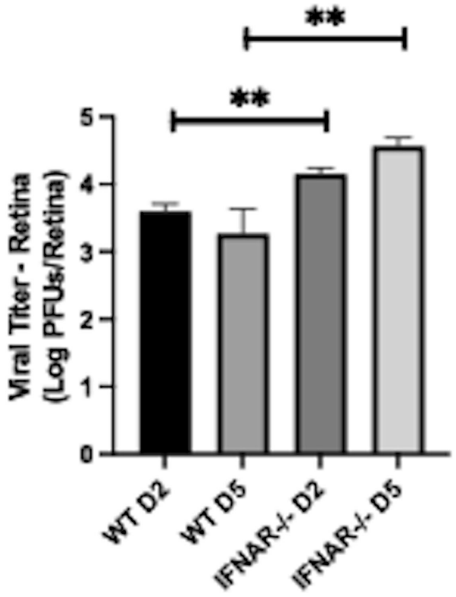

Figure 4. Loss of IFN signaling results in comprised viral containment by day 2 pi and persists. WT and IFNAR$^{-/-}$ mice were subretinally injected with 1000 PFUs of HSV-1. At two and five days pi, retinal tissue was isolated and evaluated by plaque assay. Graph represents the mean $\log_{10}$ PFUs/retina ± SEM of three independent experiments of six to nine retinas/group. $^{**}P < 0.01$; D2, day 2; D5, day 5; ns, not significant.

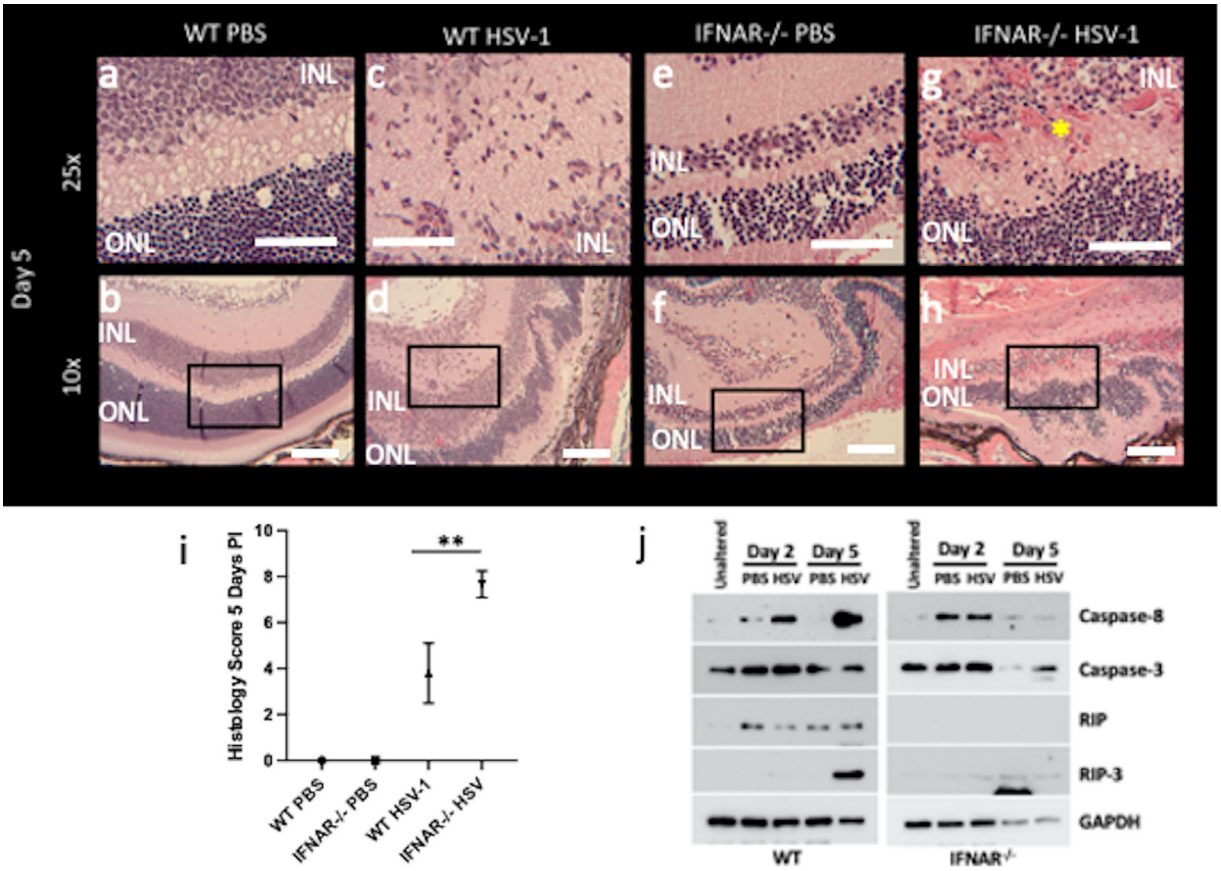

Figure 5. Loss of IFN signaling results in worse pathology. WT and IFNAR$^{-/-}$ mice were subretinally injected with PBS or 1000 PFUs of HSV-1. Five days pi, eyes were isolated, fixed, and H&E stained. (**a-h**) Top images are ×25 of area of black box in magnification ×10 images (*bottom*). WT and IFNAR$^{-/-}$ PBS controls showed normal retinal architecture (**a, b** and **e, f**, respectively) five days pi injection. WT mice show focal areas of infiltration of microglia, changes in retinal architecture and overlying vitreous inflammation in areas of necrosis (**c, d**). IFNAR$^{-/-}$ eyes had gross disorganization of the retina, intraretinal hemorrhages (*yellow asterisk*), and dense overlying vitritis in nearly all areas of the retina (**g, h**). Pathology was scored five days pi among these groups (**i**). Results represent two independent experiments of one to three eyes per group for a total of two to six eyes/group. Western blot analysis of apoptosis and necrosis markers within the retina of WT and IFNAR$^{-/-}$ mice was then performed, and results represent two independent experiments (**j**). $^{**}P < 0.01$; INL, inner nuclear layer; ONL, outer nuclear layer. *White scale bars*: 75 µm.

These architectural changes included thinning of the inner and outer nuclear layers, recruitment of ameboid-shaped microglia, and leukocyte trafficking through the vitreous at sites of retinal necrosis (Figs. 3a, 3b). Using an adapted, previously validated histopathological scoring system for viral retinitis,[19] mice infected with HSV-1 had significantly worse ocular pathology than PBS controls five days pi (Fig. 3c). These results were supported by immunofluorescence staining in which many microglia were identified within areas of HSV antigen and showed co-staining with HSV-1 antigen within these areas five days pi (Fig. 3d). This immunofluorescent co-localization was not seen in uninfected areas of the same retina five days pi (Fig. 3e).

An Absence of Type I IFN Signaling Leads to Loss of Viral Containment and Worse Tissue Pathology

Type I IFNs are cytokines that bind to a heterodimeric receptor to activate critical antiviral mediators and pathways.[1] We and others have shown that loss of IFN signals is critical in both directly and indirectly inhibiting viral spread, driving critical chemokine production, and priming adaptive immunity.[15,20] To evaluate whether the loss of IFN signaling would result in comprised local viral containment within the retina as seen in other tissues,[15–17,20] mice lacking the type I IFN receptor (IFNAR$^{-/-}$) abolishing all downstream signaling were infected with 1000 PFUs of HSV-1 and compared to WT controls. IFNAR$^{-/-}$ mice had higher viral titers by day 2 pi and had significantly higher viral titers than WT controls five days pi (Fig. 4). To assess whether increasing viral titers resulted in local tissue changes, retinal histopathology was compared between IFNAR$^{-/-}$ mice and WT controls. An increase in virus was associated with significantly worsening of retinal pathology with gross disorganization of the retina, diffuse intraretinal hemorrhages (Fig. 5g, yellow asterisk), and loss of the underlying retinal pigment epithelium in IFNAR$^{-/-}$ mice not seen in WT or PBS controls (Figs. 5a–h). Histopathological scoring confirmed significantly worse retinal changes in IFNAR$^{-/-}$ mice than WT and controls 5 days pi (Fig. 5i). Cell death, more specifically, necrosis, is a hallmark feature of ARN.[21] To assess whether cell death through apoptosis or necrosis was occurring in our

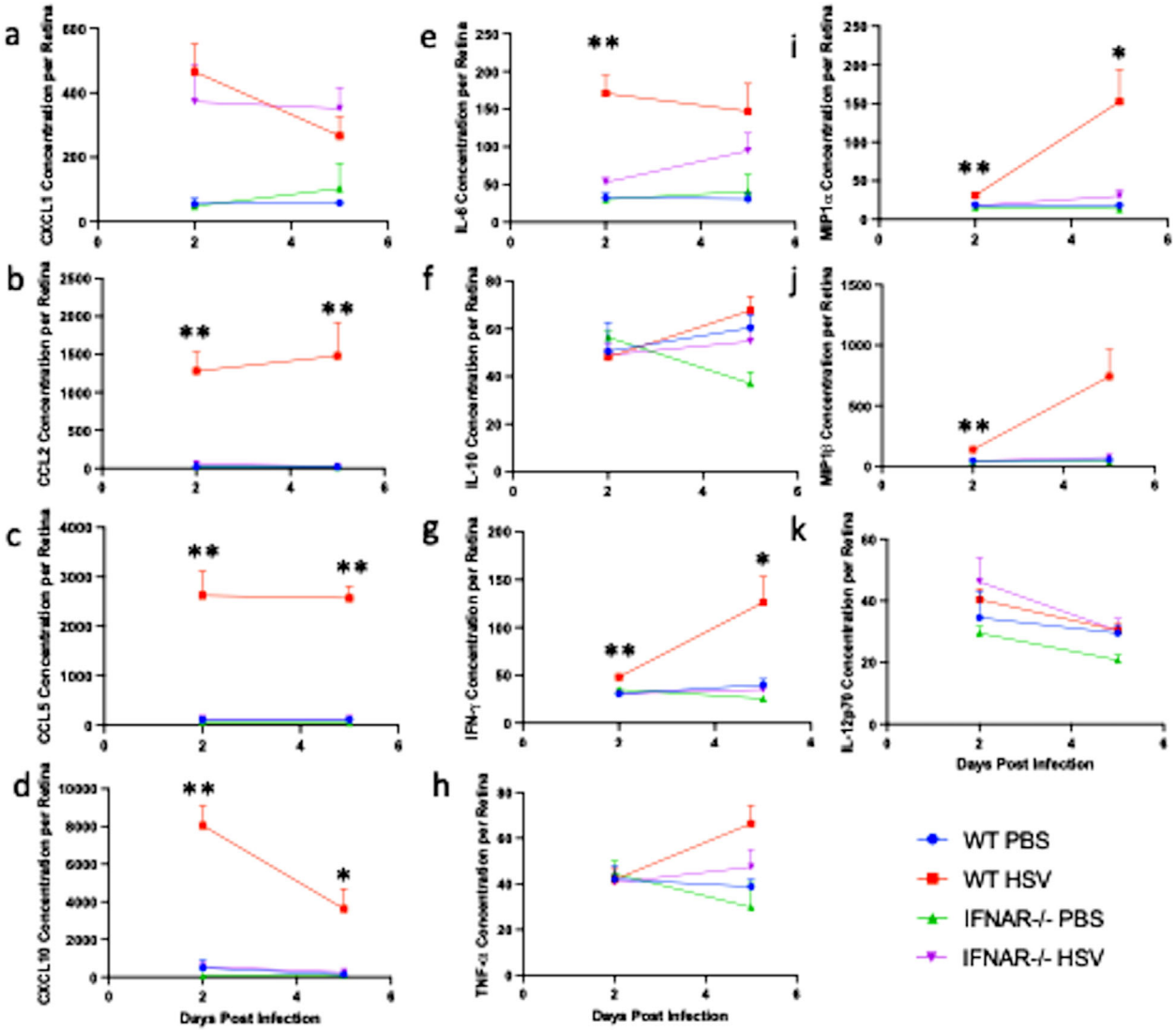

Figure 6. Loss of IFN signaling results in chemokine expression changes. WT and IFNAR$^{-/-}$ mice were subretinally injected with PBS or 1000 PFUs of HSV-1. Five days pi, retinas were isolated, and chemokine concentrations were compared (**a-k**). Results represent three independent experiments of one to four eyes per group for a total of two to eight eyes/group and are plotted as the mean concentration (pg/mg) ± standard error of the mean. $^{**}P < 0.01$.

model, protein concentrations of known cell death pathways were evaluated including Caspase-3, Caspase-8, receptor-interacting protein (RIP), and receptor-interacting protein kinase 3 (RIP3).[22] Caspase-8 and RIP3 protein concentrations increased from day 2 to day 5 pi in WT mice and were higher than PBS controls at the same time points (Fig. 5j). RIP levels remained relatively constant over time in WT mice subretinally-injected with PBS or HSV-1 but elevated compared to uninjected mice (Fig. 5j). This was in contrast to IFNAR$^{-/-}$ mice in which Caspase-3 and Caspase-8 were upregulated within 2 days of injection, whether that be with PBS or HSV-1 (Fig. 5j). At day 5 pi. Caspase-3 concentrations were higher in IFNAR$^{-/-}$ infected mice than PBS controls (Fig. 5j). RIP could not be detected in IFNAR$^{-/-}$ mice, and RIP3 was higher two days pi than controls (Fig. 5j).

An Absence of Type I IFN Signaling Leads to Changes in Chemokine Expression After Infection

We then wanted to examine what role type I IFN signals had in regulating chemokine production as well as compare our model to the von Szily mouse model and human chemokine levels. As such, we selected several chemokines that are upregulated in mice or humans (CCL2, CCL5, CXCL10, MIP-1a, MIP-1b, IL-6, and IL-10).[6,23] Most of these same cytokines were significantly elevated within the retina of WT mice when compared to IFNAR$^{-/-}$ mice and controls at two or five days pi (Figs. 6a–k). Furthermore, a chemokine that is not upregulated in humans (IL-12p70) and a chemokine shown to be upregulated during corneal HSV-1 infection (CXCL1) were not statistically different among the groups (Fig. 6a).

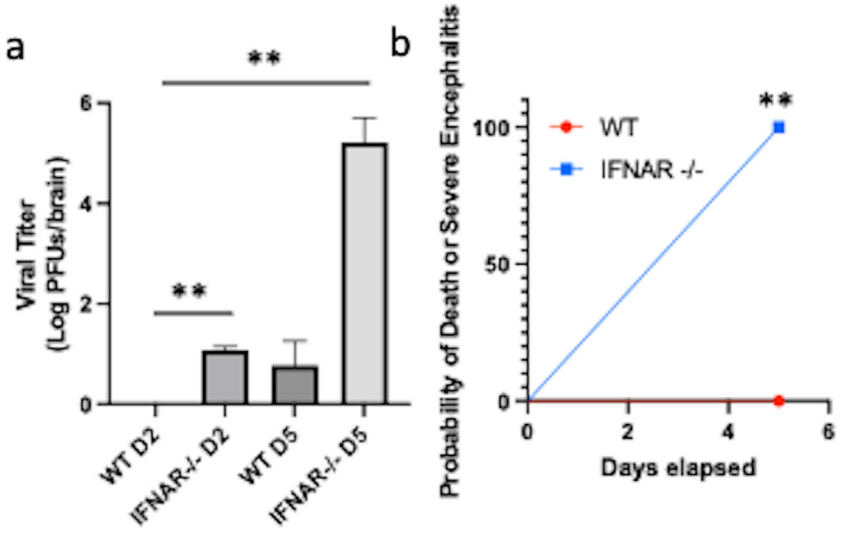

Figure 7. HSV-1 dissemination into the brain to cause encephalitis. WT and IFNAR$^{-/-}$ mice were subretinally injected with 1000 PFUs of HSV-1. At two and five days pi, brain tissue was isolated and evaluated by plaque assay. Graphs represent three independent experiments of the $\log_{10}$ PFUs/retina ± SEM (six to nine mice/group). $^{**}P < 0.01$; D2, two days after infection; D5, five days after infection.

Type I IFN Signals Prevent Viral Spread Into the Central Nervous System

To evaluate what effect the loss of local viral containment had on HSV-1 spread, viral titer two and five days pi was evaluated in the brain of WT and IFNAR$^{-/-}$ mice. By day 2 pi, virus could be detected in the cerebrum of IFNAR$^{-/-}$ mice (Fig. 7a). No virus could be detected in any WT mouse two days pi (five of five) but was detected in 100% of IFNAR$^{-/-}$ mice (four of four) at this time point. The significant difference in viral titer was only amplified by day 5 pi between WT and IFNAR$^{-/-}$ mice (Fig. 7a). The higher viral titers seen in the brain of IFNAR$^{-/-}$ mice correlated with a significantly higher rate of severe encephalitis or death by day 5 pi in IFNAR$^{-/-}$ mice than WT (Fig. 7b).

Conclusions

In the present investigation, we found that subretinal injection of HSV-1 in mice resulted in viral retinitis reminiscent of human disease histologically and observationally. Additionally, infectious virus was readily isolated from the retina. This mouse model of human disease has several potential applications, including improving our understanding of clinical ophthalmic imaging and innate immunity within the retina. Serial, in vivo imaging with histopathology will improve our understanding of the changes seen on OCT and may help identify specific OCT changes with ARN that could be used in earlier diagnosis.

Although type I IFNs are critical in local control of HSV-1, as we and others have shown, and are produced acutely after the development of ARN in mice,[10,17,20,24] their role in prohibiting viral dissemination is essential as seen by detection of virus within brain tissue within two days pi and the high rates of encephalitis in IFNAR$^{-/-}$ mice in our study. Taken together, these results support our prior work within the cornea, regional lymph nodes, and vaginal mucosa in which a loss of type I IFN signals results in more rapid viral spread to adjacent and distal tissues including the blood and brain.[15–17] The antiviral effect of type I IFNs is multifaceted in that these cytokines induce antiviral protein production, drive specific chemokine signals to promote leukocyte trafficking to sites of infection, and prime adaptive immunity also seen within our study.[15,20,25] The retina, much like the brain, is a nonregenerative, sensitive neurological tissue in which inflammation likely incites both a productive and destructive HSV-1–associated immunological response.[1] A better understanding of the immune response within the retina could be used to improve visual outcomes with targeted therapies to promote viral containment but reduce associated neuropathology.

Studies using the von Szily model have shown a broad upregulation of chemokines and cytokines both locally and systemically and the development of a virus-induced, delayed hypersensitivity reaction in genetically susceptible mice.[10,11,23] This broad upregulation of inflammatory proteins within the aqueous humor, vitreous, and serum has been confirmed in patients with the disease.[6,7] Chemokine profiles within our mouse model mirrored that of humans and those of prior mouse models of ARN.[6,23] This supports our prior work in other tissues in which the loss of type I IFN signaling results in aberrant chemokine production, most notably CCL2, which has been shown to be regulated by an upstream type I interferon-sensitive response element; however, the chemokine profile is specific to the retina because there was no significant difference in CXCL1 levels within the retina of WT and IFNAR$^{-/-}$ mice as seen in other tissues.[15,20] Furthermore, this would suggest that findings within other structures of the eye (e.g., cornea) cannot be extrapolated to the retina emphasizing the need for research focused on retinal immunology. Unfortunately, the innate immune response that drives the production of these inflammatory proteins within the retina is currently unknown in both mice and humans. Additionally, the role of host cell apoptosis and necrosis to limit HSV infection and retinal damage during ARN is unclear. In mouse models of cytomegalovirus retinitis, there is activation of multiple cell death pathways including necroptosis, pyroptosis, and apop-

Investigative Ophthalmology & Visual Science

tosis pathways.[26] In our model, we found increased levels of Caspase-3, Caspase-8, RIP, and RIP3 in WT mice, suggesting activation of multiple cell death pathways within our model as well (Fig. 5j). In mouse models of herpetic encephalitis, RIP3-mediated necroptosis restricts virus replication within the cornea and brain.[27] The role of activation of apoptosis and necroptosis in our model is unclear at this time. There are several advantages of our model compared to the historical von Szily model despite the more difficult technical challenges of a subretinal injection in mice. The advantages include a more focal retinal infection thereby reducing associated immunological noise from surrounding tissues, a more accurate time course (von Szily model has been found to have two waves of viral spread into the contralateral eye because of how the virus spreads, either through parasympathetic pathways or the optic nerve), a wider range of innate knock out mice available (von Szily model requires the use of Balb/c mice or rabbits due to inherent resistance of C57Bl/6J mice), and a closer representation of the clinical course.[28–30] The lack of knockout strains available on the BALB/c background have limited innate immune research of the retina. A recent case report and review of the literature emphasized the paucity of a von Szily presentation in humans with a total of 11 reported cases despite a yearly incidence of 0.63 cases/1 million people in the United Kingdom and, if extrapolated to the U.S. population, would be estimated to represent 210 new cases per year.[12,31] Thus clinically, a von Szily reaction is the exception, not the norm.

Last, recent advances in ophthalmology have led to a rapidly expanding field of gene therapy. Retinal dystrophies associated with loss of function mutations in *RPE65* can now be treated with adeno-associated virus-based gene therapy (Voretigene neparvovec).[32] This medical breakthrough has now seen other gene therapy–based clinical trials for various inherited retinal dystrophies commence. Not surprisingly, there is increasing evidence that these viral vectors can induce gene therapy associated uveitis in which both local and systemic immune responses are activated by toll-like receptor-2 and -9, neutralizing antibodies, and transgene-specific T-cell responses despite treatment with corticosteroids.[33,34] Unfortunately, the innate immune response to viral infection within the retina is poorly understood despite its importance in infections and inflammatory and degenerative diseases.[35] Our model, we hope, can be used to begin to unravel the immune response within the retina to viral vectors as well. Because of ocular immune privilege of the anterior chamber and vitreous, basic immunological concepts and reactions may not be pertinent within the eye and shape local responses to a pathogen differently than seen in other organs.[36–38] Thus improving our understanding of innate and adaptive immunity to viruses within the retina could improve typically poor visual outcomes with viral infections of the retina such as ARN but may also enhance gene therapy vector efficacy and identify therapeutic targets to slow retinal degenerative disorders.[35]

Acknowledgments

The authors thank Bing X. Ross, PhD, at the University of Michigan for teaching the authors how to perform subretinal injections in mice and Dan J.J. Carr, PhD, at the University of Oklahoma Health Sciences Center for providing the HSV-1 McKrae used throughout this study. Last, the authors thank Richard D. Dix, PhD, at Georgia State University for his thoughtful discussion and evaluation of our manuscript.

Supported by the Knights Templar Eye Foundation career starter grant, the IDeA Clinical and Translational Research Early Career Investigator Program, and startup funds provided by UNMC.

Disclosure: **S. Fan**, None; **J.H. Yoo**, None; **G. Park**, None; **S. Yeh**, None; **C.D. Conrady**, None

References

1. Conrady CD, Drevets DA, Carr DJJ. Herpes simplex type I (HSV-1) infection of the nervous system: is an immune response a good thing? *J Neuroimmunol*. 2010;220:1–9.
2. Kopplin LJ, Thomas AS, Cramer S, et al. Long-term surgical outcomes of retinal detachment associated with acute retinal necrosis. *Opht Surg Lasers Img Retina*. 2016;47:660–664.
3. Silva RA, Berrocal AM, Moshfeghi DM, Blumenkranz MS, Sanislo S, Davis JL. Herpes simplex virus type 2 mediated acute retinal necrosis in a pediatric population: case series and review. *Graefes Arch Clin Exp Ophthalmol*. 2013;251:559–566.
4. Schoenberger SD, Kim SJ, Thorne JE, et al. Diagnosis and treatment of acute retinal necrosis: a report by the American Academy of Ophthalmology. *Ophthalmology*. 2017;124:382–392.
5. Hadden PW, Barry CJ. Herpetic encephalitis and acute retinal necrosis. *N Engl J Med*. 2002;347:1932–1932.
6. Fukunaga H, Kaburaki T, Shirahama S, et al. Analysis of inflammatory mediators in the vitreous humor of eyes with pan-uveitis according to aetiological classification. *Sci Rep*. 2020;10:2783.
7. De Visser L, de Boer JH, Rijkers GT, et al. Cytokines and chemokines involved in acute retinal necrosis. *Invest Ophthalmol Vis Sci*. 2017;58:2139–2151.
8. Zheng M, Fields MA, Liu Y, Cathcart H, Richter E, Atherton SS. Neutrophils protect the retina of the injected eye from infection after anterior chamber inoculation of HSV-1 in BALB/c mice. *Invest Ophthalmol Vis Sci*. 2008;49:4018–4025.
9. Von Szily A. Experimental endogenous transmission of infection from bulbus to bulbus. *Klin Monatsbl Augenheilkd*. 1924;75:593–602.
10. Cathcart HM, Zheng M, Covar JJ, Liu Y, Podolsky R, Atherton SS. Interferon-gamma, macrophages, and virus spread after HSV-1 injection. *Invest Ophthalmol Vis Sci*. 2011;52:3984–3993.
11. Hemady R, Tauber J, Ihley TM, Opremcak EM, Foster CS. Viral isolation and systemic immune responses after intracameral inoculation of herpes simplex virus type 1 in Igh-1-disparate congenic murine strains. *Invest Ophthalmol Vis Sci*. 1990;31:2335–2341.
12. Ng CC, Chen JJ, Agarwal A, Cunningham ET. Clinical course of von Szily reaction: Case report and comprehensive review of the literature. *Am J Ophthalmol Case Rep*. 2020;20:100927.
13. Ross BX, Jia L, Kong D, et al. Conditional knock out of high-mobility group box 1 (HMGB1) in rods reduces autophagy activation after retinal detachment. *Cells*. 2021;10:2010.
14. Freeman W, Schneiderman TE, Wiley CA, et al. An animal model of focal, subacute, viral retinitis. *Retina*. 1993;13:214–21.
15. Conrady CD, Thapa M, Wuest T, Carr DJJ. Loss of mandibular lymph node integrity is associated with an increase in sensitivity to HSV-1 infection in CD118-deficient mice. *J Immunol*. 2009;182:3678–3687.

Investigative Ophthalmology & Visual Science

16. Conrady CD, Zheng M, van Rooijen N, et al. Microglia and a functional type I IFN pathway are required to counter HSV-1-driven brain lateral ventricle enlargement and encephalitis. *J Immunol*. 2013;190:2807–2817.
17. Conrady CD, Halford WP, Carr DJJ. Loss of the type I interferon pathway increases vulnerability of mice to genital herpes simplex virus 2 infection. *J Virol*. 2011;85:1625–1633.
18. Conrady CD, Zheng M, Fitzgerald KA, Liu C, Carr DJJ. Resistance to HSV-1 infection in the epithelium resides with the novel innate sensor, IFI-16. *Mucosal Immunol*. 2012;5:173–183.
19. Dix RD, Cray C, Cousins SW. Mice immunosuppressed by murine retrovirus infection (MAIDS) are susceptible to cytomegalovirus retinitis. *Curr Eye Res*. 1994;13:587–595.
20. Conrady CD, Zheng M, Mandal NA, van Rooijen N, Carr DJJ. IFN-α-driven CCL2 production recruits inflammatory monocytes to infection site in mice. *Mucosal Immunol*. 2013;6:45–55.
21. Shantha JG, Weissman HM, Debiec MR, Albini TA, Yeh S. Advances in the management of acute retinal necrosis. *Int Ophthalmol Clin*. 2015;55:1–13.
22. D'Arcy MS. Cell death: a review of the major forms of apoptosis, necrosis and autophagy. *Cell Biol Int*. 2019;43:582–592.
23. Zheng M, Atherton SS. Cytokine profiles and inflammatory cells during HSV-1–induced acute retinal necrosis. *Invest Ophthalmol Vis Sci*. 2005;46:1356–1363.
24. Mikloska Z, Cunningham AL. Alpha and gamma interferons inhibit herpes simplex virus type 1 infection and spread in epidermal cells after axonal transmission. *J Virol*. 2001;75:11821–11826.
25. Al-khatib K, Williams BRG, Silverman RH, Halford W, Carr DJJ. The murine double-stranded RNA-dependent protein kinase PKR and the murine 2′,5′-oligoadenylate synthetase-dependent RNase L are required for IFN-β-mediated resistance against herpes simplex virus type 1 in primary trigeminal ganglion culture. *Virology*. 2003;313:126–135.
26. Chien H, Dix RD. Evidence for multiple cell death pathways during development of experimental cytomegalovirus retinitis in mice with retrovirus-induced immunosuppression: apoptosis, necroptosis, and pyroptosis. *J Virol*. 2012;86:10961–10978.
27. Guo H, Koehler HS, Mocarski ES, Dix RD. RIPK3 and caspase 8 collaborate to limit herpes simplex encephalitis. *PLOS Pathogens*. 2022;18:e1010857.
28. Nguyen QD, Uy HS, Merchant A, et al. Effect of Fas and Fas ligand deficiency in resistance of C57BL/6 mice to HSV-1 keratitis and chorioretinitis. *Invest Ophthalmol Vis Sci*. 2001;42:2505–2509.
29. Atherton SS, Streilein JW. Two waves of virus following anterior chamber inoculation of HSV-1. *Invest Ophthalmol Vis Sci*. 1987;28:571–579.
30. Kielty D, Cousins SW, Atherton SS. HSV-1 retinitis and delayed hypersensitivity in DBA/2 and C57BL/6 mice. *Invest Ophthalmol Vis Sci*. 1987;28:1994–1999.
31. Cochrane TF, Silvestri G, McDowell C, Foot B, McAvoy CE. Acute retinal necrosis in the United Kingdom: results of a prospective surveillance study. *Eye*. 2012;26:370–378.
32. Russell S, Bennett J, Wellman JA, et al. Efficacy and safety of voretigene neparvovec (AAV2-hRPE65v2) in patients with RPE65-mediated inherited retinal dystrophy: a randomised, controlled, open-label, phase 3 trial. *Lancet*. 2017;390:849–860.
33. Bucher K, Rodríguez-Bocanegra E, Dauletbekov D, Fischer MD. Immune responses to retinal gene therapy using adeno-associated viral vectors—Implications for treatment success and safety. *Progr Retinal Eye Res*. 2021;83:100915.
34. Verdera HC, Kuranda K, Mingozzi F. AAV Vector Immunogenicity in humans: a long journey to successful gene transfer. *Mol Ther*. 2020;28:723–746.
35. Fukuda S, Narendran S, Varshney A, et al. Alu complementary DNA is enriched in atrophic macular degeneration and triggers retinal pigmented epithelium toxicity via cytosolic innate immunity. *Sci Adv*. 2021;7:eabj3658.
36. Streilein JW. Anterior chamber associated immune deviation: the privilege of immunity in the eye. *Surv Ophthalmol*. 1990;35:67–73.
37. Streilein JW, Ksander BR, Taylor AW. Immune deviation in relation to ocular immune privilege. *J Immunol*. 1997;158:3557.
38. Eichhorn M, Horneber M, Streilein JW, Lutjen-Drecoll E. Anterior chamber-associated immune deviation elicited via primate eyes. *Invest Ophthalmol Vis Sci*. 1993;34:2926–2930.

Investigative Ophthalmology & Visual Science